The American Journal of Pathology, Vol. 181, No. 4, October 2012

http://dx.doi.org/10.1016/j.ajpath.2012.06.014

Animal Models

A Novel Animal Model for Pseudoxanthoma Elasticum

The KK/HlJ Mouse

Qiaoli Li,* Annerose Berndt,† Haitao Guo,*
John P. Sundberg,‡ and Jouni Uitto*

From the Department of Dermatology and Cutaneous Biology, Jefferson Medical College, Philadelphia, Pennsylvania; the Division of Pulmonary, Allergy and Critical Care Medicine,† Department of Medicine, University of Pittsburgh, Pittsburgh, Pennsylvania; and The Jackson Laboratory,‡ Bar Harbor, Maine*

Pseudoxanthoma elasticum is a multisystem ectopic mineralization disorder caused by mutations in the *ABCC6* gene. A mouse model with targeted ablation of the corresponding gene (*Abcc6*^{tm1Jfk}) develops ectopic mineralization on the dermal sheath of vibrissae as biomarker of the progressive mineralization disorder. Survey of 31 mouse strains in a longitudinal aging study has identified three mouse strains with similar ectopic mineralization of the vibrissae, particularly the KK/HlJ strain. We report here that this mouse strain depicts, in addition to ectopic mineralization of the dermal sheath of vibrissae, mineral deposits in a number of internal organs. Energy dispersive X-ray analysis and topographic mapping found the presence of calcium and phosphate as the principal ions in the mineral deposits, similar to that in *Abcc6*^{tm1Jfk} mice, suggesting the presence of calcium hydroxyapatite. The mineralization was associated with a splice junction mutation at the 3′ end of exon 14 of the *Abcc6* gene, resulting in a 5-bp deletion from the coding region and causing frame-shift of translation. As a consequence, essentially no Abcc6 protein was detected in the liver of the KK/HlJ mice, similar to that in *Abcc6*^{tm1Jfk} mice. Collectively, our studies found that the KK/HlJ mouse strain is characterized by ectopic mineralization due to a mutation in the *Abcc6* gene and therefore provides a novel model system to study pseudoxanthoma elasticum. ***(Am J Pathol 2012, 181:1190–1196; http://dx.doi.org/10.1016/j.ajpath.2012.06.014)***

Pseudoxanthoma elasticum (PXE), an autosomal recessive disorder, is characterized by ectopic mineralization of soft connective tissues in the skin, the eyes, and the cardiovascular system.[1,2] Histopathology of the affected skin in patients with PXE found accumulation of pleiomorphic elastotic material with propensity for aberrant mineralization, the mineral deposits consisting of calcium hydroxyapatite. In the eye, an elastin rich membrane, the Bruch's membrane, becomes mineralized, resulting in breakage (angioid streaks), and neovascularization of the retina can lead to progressive loss of visual acuity and occasionally blindness.[3] The arterial blood vessels show mineralization, resulting in hypertension, intermittent claudication, and occasionally rupture of vessels of the internal organs, predominantly of the gastric arteries.[4] This multisystem disorder is most frequently caused by mutations in the ATP-binding cassette, subfamily C (CFTR/MRP), member 6 (*ABCC6*) gene that encodes a putative efflux transporter protein, ABCC6, expressed primarily in the liver and to a lesser extent in the kidneys.[2,5] The pathomechanistic details leading from mutations in the *ABCC6* gene to peripheral connective tissue mineralization are currently unknown, and specifically, the nature of the substrate(s) for the ABCC6 transporter remains to be identified.[6,7] It has been postulated, however, that physiologically the transported molecules serve in

Supported by NIH grants R01AR28450 and R01AR55225 (J.U.) and AG25707 and CA89713 (J.P.S.), Ellison Medical Foundation (J.P.S.), Dermatology Foundation Research Career Development Award (Q.L.), a fellowship by the Parker B. Francis Foundation (A.B.). Confocal imaging of subcellular localization of the mouse Abcc6 protein was performed in the Bioimaging Facility of the Kimmel Cancer Center at Thomas Jefferson University (National Institutes of Health Cancer Center Core grant 5 P30 CA-56036). The Jackson Laboratory Shared Scientific Services were supported in part by a Basic Cancer Center Core Grant from the National Cancer Institute (CA34196).

Accepted for publication June 18, 2012.

A guest editor acted as editor-in-chief for this manuscript. No person at Thomas Jefferson University was involved in the peer review process or final disposition of this article.

Supplemental material for this article can be found at *http://ajp.amjpathol.org* or at *http://dx.doi.org/10.1016/j.ajpath.2012.06.014*.

Address reprint requests to Jouni Uitto, M.D., Ph.D., Department of Dermatology and Cutaneous Biology, Jefferson Medical College, 233 S. 10th Street, Suite 450 BLSB, Philadelphia, PA 19107. E-mail: jouni.uitto@jefferson.edu.

the circulation as antimineralization factors under normal calcium and phosphate homeostasis, and their absence in PXE allows progressive mineralization to ensue.[2,7,8]

Understanding of the processes of mineralization in PXE has been aided by development of *Abcc6* knockout mice (*Abcc6*^{tm1JfK}) by targeted ablation of the corresponding gene, and these mice recapitulate the genetic, histopathologic, and ultrastructural features of PXE.[9,10] Specifically, this mouse model shows late-onset mineralization, beginning at 5 to 6 weeks of age on mixed C57BL/6J and 129S1/SvImJ genetic background when fed standard rodent laboratory diet.[9,11] The mineralization process also affects the same organ systems as in patients with PXE, that is, the skin, the eyes, and the arterial blood vessels. Use of these mice in skin grafting and parabiosis experiments has established that PXE is a metabolic disorder,[12,13] and *Abcc6*^{tm1JfK} mice have also served as a preclinical platform to develop potential treatment modalities for this, currently intractable, disorder.[14] The mouse studies have also found that manipulation of the diet can significantly alter the onset and severity of the pathologic findings,[15,16] and breeding *Abcc6*^{tm1JfK} mice on different genetic backgrounds modulates the age of onset and the degree of mineralization.[17]

A characteristic finding in the *Abcc6*^{tm1JfK} mice is mineralization of the dermal sheath of vibrissae, the earliest site of mineralization, and quantitation of the degree of mineralization by computerized morphometric analysis and by direct chemical assay of calcium and phosphate has been shown to serve as an early, reliable biomarker of the progression of the entire mineralization process.[11] Recently, as part of a longitudinal aging study conducted at The Jackson Laboratory (Bar Harbor, ME), three different mouse strains, KK/HlJ, 129S1/SvImJ, and RIIIS/J, were found to develop mineralization of the dermal sheath of vibrissae by 20 months of age, similar to that noted in *Abcc6*^{tm1JfK} mice.[18] Among these strains, the KK/HlJ mice had the most frequent diagnosis of tissue mineralization. In this study, we have examined the KK/HlJ mouse strain in detail for the onset of mineralization and the mineral composition, and we report a splice junction mutation in the *Abcc6* gene, with subsequent reduction in the gene expression at the protein level.

Materials and Methods

Mice

The KK/HlJ mice (JR no. 2106) were initially part of a large-scale aging study by The Jackson Aging Center, for which details have been described elsewhere.[18] The breeding facilities and the mouse rooms were regulated on a 12-hour light/12-hour dark cycle and were maintained at an ambient temperature of 21°C to 23°C. Mice were allowed *ad libitum* access to acidified water (pH 2.8 to 3.2) and placed on rodent diet (LabDiet 5K52; PMI Nutritional International, Bentwood, MO). The mice were euthanized at different ages by CO_2 asphyxiation with the use of methods approved by the American Veterinary Medical Association and subjected to necropsy. All protocols were reviewed and approved by The Jackson Laboratory Institutional Animal Care and Use Committee. Mouse handling and care were followed according to animal welfare policies of the Public Health Service.

Abcc6^{tm1JfK} mice, a model for PXE, were developed by targeted ablation of the mouse *Abcc6* gene.[9] *Abcc6*^{tm1JfK} mice were made congenic on C57BL/6J background (10 generations). These mice were housed in the Animal Facility of Thomas Jefferson University where they were maintained in a climate-controlled environment with free access to water and a 12-hour light/dark cycle. Mice were placed on the standard rodent diet (Laboratory Autoclavable Rodent Diet 5010; PMI Nutritional International). This study was approved by the Institutional Animal Care and Use Committee of Thomas Jefferson University.

Histologic Analysis

Complete necropsies were performed after euthanizing the mice.[19] For histopathologic analysis of mineralization, biopsies from muzzle skin containing vibrissae as well as internal organs were fixed in 10% phosphate-buffered formalin and embedded in paraffin. Paraffin sections (6 μm) were stained with H&E, alizarin red, or von Kossa with the use of standard methods. Sections containing mineral deposits in muzzle skin were used for analysis by energy dispersal X-ray elemental analyzer (EDAX) and for topographic mapping (RADAR).

EDAX of Elements Composition

Paraffin sections of biopsies from muzzle skin containing vibrissae were mounted onto carbon carriers. Specimens were imaged and analyzed for elemental composition in a JEOL-T330A scanning electron microscope (JEOL Ltd., Tokyo, Japan) fitted with an EDAX analyzer. X-ray maps of coated samples and RADAR mapping of calcium and phosphate were collected by Thermo Scientific NSS software version 2.3 (West Palm Beach, FL).

RNA Extraction and RT-PCR

Total RNA from mouse liver was isolated with Trizol reagent (Invitrogen, Carlsbad, CA) followed by a RNeasy Mini Kit (Qiagen, Valencia, CA). Total RNA was treated with DNase I on minicolumns to eliminate genomic DNA. First-strand cDNA was synthesized with reverse transcriptase and random hexamer primers (Invitrogen), with 2 μg of RNA in each reaction. For the amplification of the PCR product flanking the 5-bp deletion in the *Abcc6* gene in KK/HlJ mice, we used primer pairs (KK-E14F: 5′-CGAGTGTCCTTTGACCGGCT-3′; KK-E15R: 5′-TGGG-CTCTCCTGGGACCAA-3′) that produce a 144-bp or 139-bp PCR fragment representing wild-type and mutant alleles, respectively. Sequencing of PCR products was performed with an Applied Biosystems 3730 Sequencer (Applied Biosystems, Foster City, CA). For the separation of the 5-bp deletion containing fragment from the wild-type cDNA, high-resolution electrophoresis was performed with a 15% MINI-PROTEAN Precast Gel (Bio-Rad,

Hercules, CA) and ethidium bromide staining. To further analyze the bands in KK/HlJ mice, the PCR product in KK/HlJ mice was subcloned into pCRII-TOPO vector with the use of TOPO TA cloning kit (Invitrogen), and the insert clones were sequenced for differences in the insert size.

The consequences of nonsynonymous sequence variants in the *ABCC6* gene to the corresponding protein function were analyzed by two independent mutation prediction programs, PolyPhen-2 (*http://genetics.bwh.harvard.edu/pph2*) and SIFT software (*http://sift.jcvi.org/www/SIFT_pid_subst_all_submit.html*).

Real-Time PCR

Real-time PCR was conducted with Power SYBR Green PCR Master Mix with the ABI Prism 7000 sequence detection system (Applied Biosystems), as described previously.[20] The amount of *Abcc6* mRNA in each RNA sample was quantified and normalized to *Gapdh* mRNA. The relative *Abcc6* expression level was calculated with the ΔΔCt method. Reaction specificity was determined by the dissociation curve and was visualized with the software Dissociation Curve 1.0 (Applied Biosystems).

IF and Image Acquisition

Mouse liver was quickly harvested, placed in Optimal Cutting Temperature compound and stored at −80°C. Immunofluorescent staining of liver samples was performed with 5-μm frozen sections. The goat polyclonal anti-Abcc6 antibody (S-20) was used to identify the mouse Abcc6 protein (Santa Cruz Biotechnology, Inc., Santa Cruz, CA). The Alexa Fluor 488 donkey anti-goat secondary antibody was used for incubation with tissue sections (Invitrogen). The sections were then followed by staining with 4 μg/mL DAPI for 5 minutes at room temperature. Coverslips were mounted onto glass microscope slides with the use of Prolong Gold Antifade Reagent (Invitrogen). Confocal images were acquired with a Carl Zeiss LSM 510 UV META inverted confocal microscopy (Carl Zeiss Microimaging, Thornwood, NY) with a Plan-Apo 63× oil immersion lens at room temperature and Zeiss AIM 4.2 SP1 software. Images were analyzed with MetaMorph version 7.6.5 (Molecular Devices, Inc., Sunnyvale, CA). Immunofluorescence (IF) data were collected from several fields of view across two independent experiments.

Statistical Analysis

The results in different groups of mice were evaluated by Student's *t*-test. Statistical significance was reached with $P < 0.05$.

Results

As part of a large-scale aging study of 31 inbred strains performed at The Jackson Laboratory, mineralization of dermal sheath of vibrissae, a characteristic feature of

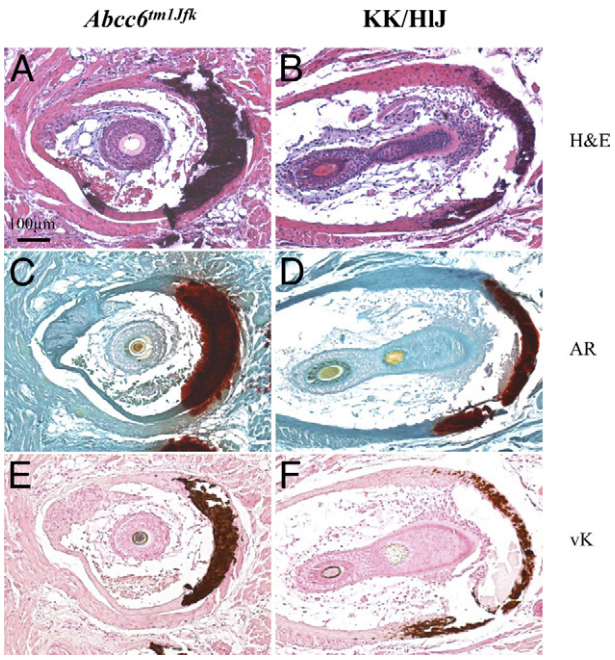

Figure 1. Ectopic mineralization of the connective tissue sheath of vibrissae in KK/HlJ mice at 6 months of age is shown in comparison with age-matched *Abcc6*^{tm1Jfk} mice. Parallel sections were stained with H&E (**A** and **B**), alizarin red (AR; **C** and **D**), or von Kossa (vK; **E** and **F**) stain. The dark red brownish color represents mineral deposits. The magnification in all frames is the same. Scale bar = 100 μm (**A**).

Abcc6^{tm1JfK} mice, was diagnosed histologically in three inbred mouse strains at 20 months of age with the use of H&E stain.[18] Among them, KK/HlJ mice were diagnosed with mineralization more frequently than 129S1/SvImJ or RIIIS/J mice. In addition to the mineralization of dermal sheath of vibrissae there was mineralization of internal organs, including heart, medium-sized arteries, lung, and retina, and was particularly severe in the KK/HlJ strain (see Supplemental Table S1 at *http://ajp.amjpathol.org*). In this study, the mineralization process was further characterized by special stains that recognize, but are not specific for, calcium and phosphate.[21] Specifically, utilization of alizarin red and von Kossa stains showed mineral deposits in the connective tissue sheath surrounding vibrissae in mice as early as 2 months of age (Figure 1, A–F). To identify the components of the mineral deposits, EDAX analysis and RADAR mapping were performed on the connective tissue capsule of the vibrissae. The results indicate prominent peaks that correspond to calcium and phosphate, and the calcium-to-phosphate ratio in KK/HlJ mice, ~2.1, was the same as that noted in *Abcc6*^{tm1JfK} mice and in endochondral bone (Figure 2A). RADAR map showed that calcium and phosphate topographically colocalized with histologically demonstrable mineral deposits, suggesting the presence of calcium phosphate complexes. Collectively, these findings suggest that the mineral deposits in KK/HlJ mice consist of calcium hydroxyapatite, similar to that in *Abcc6*^{tm1JfK} mice as recently reported by us[22] (Figure 2, A and B).

Previous haplotype analyses of KK/HlJ mice, compared with mouse strains without mineralization of connective tissue sheath of vibrissae, including C57BL/6J,

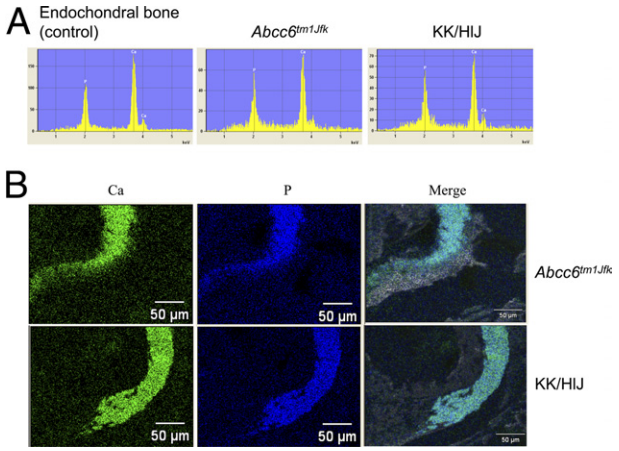

Figure 2. Mineral deposits in the dermal sheath of vibrissae in KK/HlJ mice consist of calcium and phosphate, similar to that in *Abcc6*^{tm1Jfk} mice. The ratio of calcium to phosphate is ~2.1, similar to that noted in endochondral bone as a control (**A**). RADAR mapping shows topographic colocalization of calcium (Ca) and phosphate (P) in the area corresponding to the mineralization, as visualized by scanning electron microscopy (**B**).

found two single nucleotide polymorphisms, predicting amino acid substitutions in exons 14 and 29 of the *Abcc6* gene (J.P. Sundberg, unpublished data). In this study, the nonsynonymous single nucleotide polymorphism in exon 14 was shown by sequence analysis to create a new splice donor site at the 3′ end of exon 14, similar to C3H/HeJ mice noted previously (see Discussion). As a result, there was a 5-bp deletion in the coding sequence

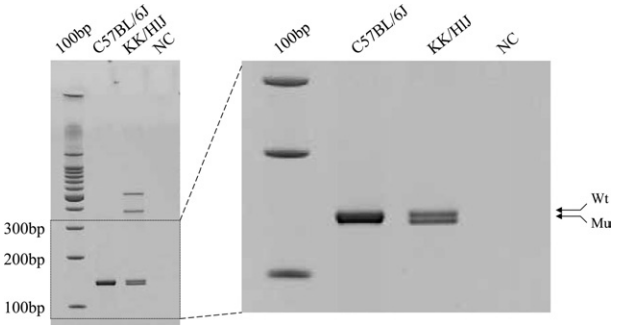

Figure 4. A 5-bp deletion in the *Abcc6* mRNA in KK/HlJ mice is shown. RT-PCR amplification of *Abcc6* mRNA with the use of primers on exon 14 upstream from the C-to-T transition mutation and on exon 15 resulted in two products, 144 bp and 139 bp, respectively, reflecting the deletion of 5 bp in the mutant mRNA. Mu, mutant; NC, negative control; Wt, wild type.

of *Abcc6*, which caused the reading of translation to be out of frame with a new premature termination codon 200 bp downstream from the site of the mutation (Figure 3). The 5-bp deletion was also found by RT-PCR, using liver *Abcc6* mRNA from KK/HlJ and C57BL/6J mice as templates on high-resolution miniprotean gel, which resulted in two bands of different mobilities in KK/HlJ mice (Figure 4). Subcloning of the PCR products in the KK/HlJ mouse indicated the presence of two inserts with different sizes, corresponding to wild-type and mutant *Abcc6* mRNA transcripts. The mutant transcript was indeed 5 bp shorter than the corresponding wild-type mRNA, as determined by direct nucleotide sequencing.

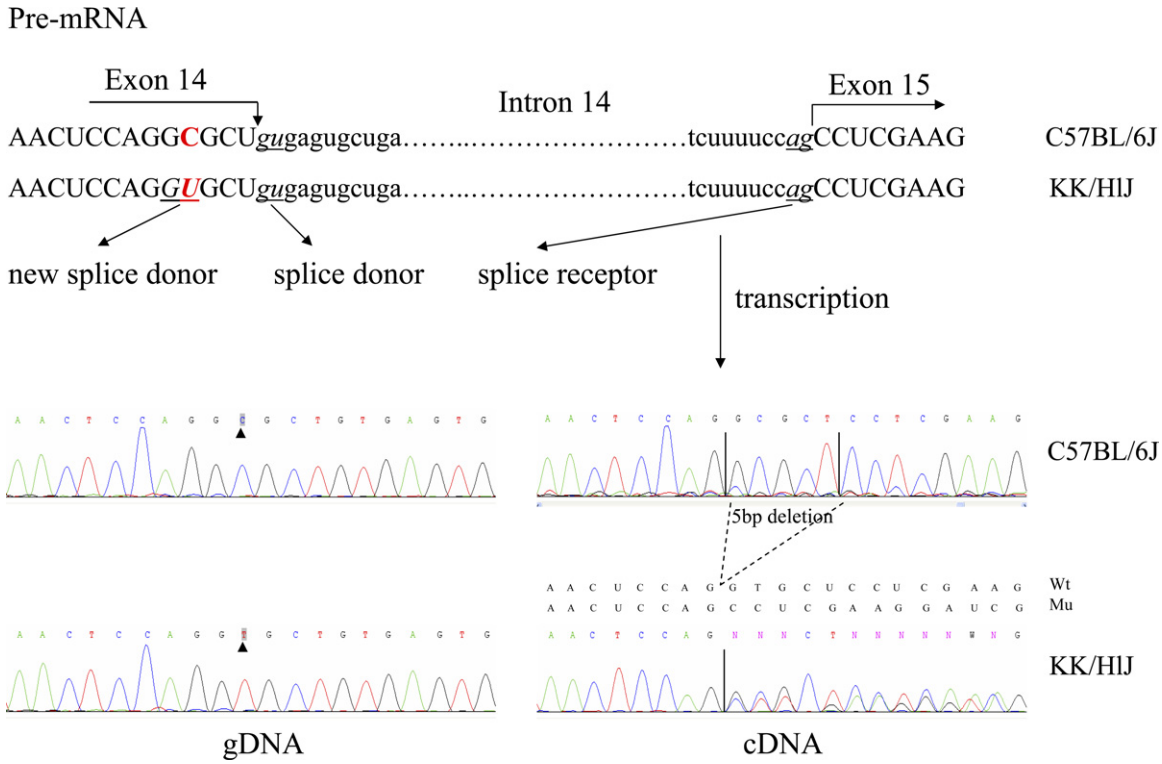

Figure 3. Sequence comparison of the KK/HlJ mice that shows ectopic mineralization and C57BL/6J mice without mineralization. Sequencing of the *Abcc6* gene at the 3′ end of exon 14 shows a C-to-T transition substitution (**arrowheads**), which in pre-mRNA is predicted to create a new splice donor site. Sequencing of the RT-PCR product (cDNA) shows a frame shift in the KK/HlJ mouse mRNA compared with the wild-type sequence in C57BL/6J. Wt, wild-type; Mu, mutant.

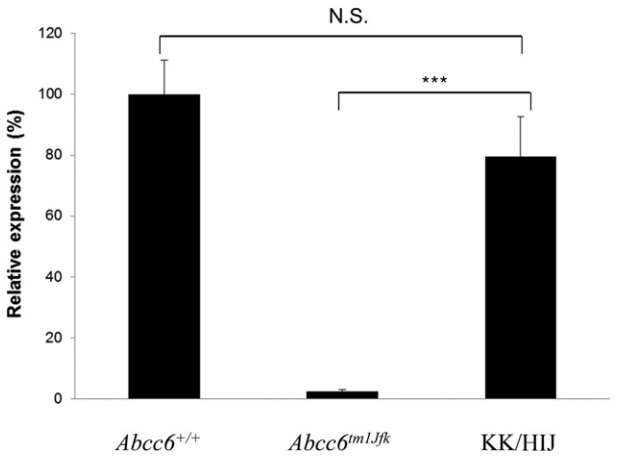

Figure 5. Quantitation of the *Abcc6* mRNA in the liver of the KK/HlJ mice in comparison with $Abcc6^{tm1Jfk}$ mice. Note that the transcript levels were reduced by ~20% in KK/HlJ mice, whereas it was completely absent in the $Abcc6^{tm1Jfk}$ mice compared with $Abcc6^{+/+}$ controls (100%). The values are mean ± SE; $n = 9$. N.S., not significant. $^{***}P < 0.001$.

In contrast, the C57BL/6J mouse product consisted only of the wild-type band (Figure 4).

The second polymorphism found in exon 29 of the *Abcc6* gene in KK/HlJ mice resulted in substitution of alanine by threonine at position 1368 (p.A1368T). This amino acid substitution was considered to be inconsequential, for two reasons. First, two independent mutation prediction programs (PolyPhen-2 and SIFT software) suggested that this amino acid substitution is "benign" and inconsequential for the protein function. Second, the p.A1368T substitution was also found in another mouse strain, PWD/PhJ, that does not show ectopic mineralization in the skin, heart, arterial blood vessels, or eye as noted in the KK/HlJ mice when examined at the age of 20 months (J.P. Sundberg, unpublished data).

To examine the consequences of the mutations in the *Abcc6* gene in KK/HlJ mice at mRNA and protein levels, mRNA quantitation as well as IF analyses were performed. Quantitative real-time PCR indicated that the mean *Abcc6* mRNA transcript level in the KK/HlJ mouse liver was 82% of that noted in the liver of wild-type mice; this difference was statistically not significant ($P = 0.602$; $n = 9$; Figure 5). In comparison, the corresponding mRNA transcript in $Abcc6^{tm1JfK}$ knockout mice was essentially undetectable, <1% of the level in wild-type mice with the primers used ($P < 0.001$; $n = 9$). To examine the expression of the *Abcc6* gene at the protein level, IF analysis of the liver from KK/HlJ mice was performed with an Abcc6-specific antibody and compared with $Abcc6^{tm1JfK}$ mice and their wild-type counterparts. As shown in Figure 6, the *Abcc6* antibody recognized protein epitopes localized on the plasma membranes of hepatocytes in control mice. In contrast, staining of the $Abcc6^{tm1JfK}$ mouse liver was entirely negative for IF, and the level of expression in KK/HlJ mice was low. Thus, in KK/HlJ mice there is a significant loss of Abcc6 protein in the liver.

The mineralization of the dermal sheath of vibrissae has been shown in $Abcc6^{tm1JfK}$ mice to be associated with mineralization of a number of internal organs.[9] In this study, we also examined the KK/HlJ mice for internal organ involvement through necropsy of these mice at different ages. Histopathologic survey found the presence of ectopic mineral deposits in a number of tissues in KK/HlJ mice (see Supplemental Table S1 at *http://ajp.amjpathol.org*). Particularly prevalent in 20-month-old mice was the presence of mineral deposits in the arterial blood vessels, heart, and lungs. Thus, the mineralization of the dermal sheath of vibrissae in the KK/HlJ mice also reflects the involvement of internal organs by the mineralization processes.

Discussion

PXE is a prototype of ectopic heritable mineralization disorders with extensive multisystem involvement by dystrophic mineralization.[1,2] This disorder is caused by mutations in the *ABCC6* gene, encoding an efflux transporter expressed primarily in the liver.[2,5] The pathomechanistic details that lead from *ABCC6* mutations to ectopic peripheral mineralization are currently unknown, but considerable progress toward understanding the nature of this disorder has been made by development of a mouse model for PXE through targeted ablation of the mouse *Abcc6* gene.[9,10] In this study, we characterized a novel mouse model for PXE. Specifically, as part of a large-scale aging study that examined 31 strains of mice, it was noted that some strains depicted ectopic mineralization of the dermal sheath of vibrissae, similar to that previously noted in the $Abcc6^{tm1JfK}$ mice. Among the strains initially described, the degree of mineralization of dermal sheath of vibrissae was highest in KK/HlJ inbred mice. This strain originated from Japan about a half century ago,[23] and it is currently distributed by The Jackson Laboratory where the mice have been inbred for >64 generations. In this study, we found that the KK/HlJ mice are characterized, in addition to mineralization of the dermal sheath of vibrissae, by mineral deposits in a number of internal organs, similar to those noted in $Abcc6^{tm1JfK}$ mice.[9] The mineral deposits were shown to contain calcium and phosphate in a ratio similar to that in endochondral bone, suggesting that the mineral deposits consist of calcium hydroxyapatite similar to the mineralized lesions in patients

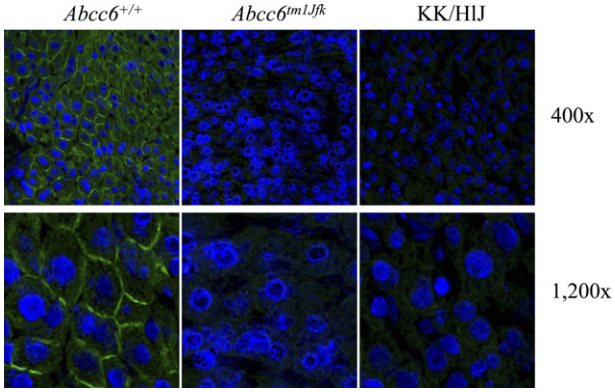

Figure 6. IF analysis of Abcc6 protein in the liver of KK/HlJ mice in comparison with $Abcc6^{tm1JfK}$ mouse and its wild-type counterpart ($Abcc6^{+/+}$). The magnifications in frames are shown on the right side of the figure.

with PXE.[24] These observations further validate the KK/HlJ mouse as a model for human PXE.

We have previously detected the presence of two nonsynonymous single nucleotide polymorphisms in the *Abcc6* gene, and here we showed that these polymorphisms are accompanied with mineralization of the connective tissue sheath of vibrissae. We specifically found that a C-to-T substitution in KK/HlJ in exon 14 (rs32756904) creates a novel splice donor site, resulting in miss-splicing and formation of an mRNA transcript that is devoid of 5 bp at the end of the exon 14 coding sequence. This results in frame shift of translation and formation of a premature termination codon 200 bp downstream from the site of the nucleotide substitution. We found that this genetic defect results in essentially complete absence of the corresponding protein in the liver of KK/HlJ mice, similar to that in *Abcc6*^{tm1JfK} mice. Quantitative real-time RT-PCR of the *Abcc6* mRNA transcript in KK/HlJ showed ~80% level of expression as compared with the corresponding wild-type control. This is in contrast to the findings in the *Abcc6*^{tm1JfK} mice, which have complete absence of the corresponding mRNA transcripts. This difference is likely to reflect consequences of the different genetic lesions between the *Abcc6*^{tm1JfK} and KK/HlJ mice for nonsense-mediated mRNA decay.[25] Nevertheless, the *Abcc6* mRNA detected in the liver of KK/HlJ mice contains a frame shift and a premature termination codon of translation, explaining the absence of the corresponding protein.

In addition to mineralization of the dermal sheath of vibrissae, the KK/HlJ mice exhibited extensive mineralization of a number of internal organs, including vascular and cardiac tissues. In particular, there is considerable epicardial and myocardial mineralization in KK/HlJ mice, similar to dystrophic cardiac calcinosis.[26–29] It should be noted that cardiac mineralization developed in the KK/HlJ mice spontaneously under the experimental conditions used, including standard mouse diet. There are four quantitative trait loci of dystrophic cardiac calcinosis (Dyscalc 1 to 4), and one of them (Dyscalc 1) is located on mouse chromosome 7, in the region containing the *Abcc6* gene.[29] The mice showing considerable cardiac mineralization were a cross from C57BL/6J and C3H/HeJ, when fed an experimental, high-fat diet.[29] C3H/HeJ mouse has also been shown to harbor the same C-to-T transition mutation in the *Abcc6* gene as found in the KK/HlJ mice, but the dystrophic cardiac calcinosis phenotype was noted only after freeze-thaw injury of the cardiac tissue.[30] The cardiac mineralization phenotype in KK/HlJ mice has also been suggested to be caused by the presence of a functional retroposon, *Lamr1*.[31] Collectively, these data suggest that tissue mineralization, including dystrophic cardiac calcinosis, can result from genetic lesions in a number of genes and that the mineralization process as a result of mutations in the *Abcc6* gene can be modulated by modifier genes and environmental factors, including the diet.[2,14–17] These conclusions are consistent with observations in patients with PXE phenotypes, which can also result from mutations in genes other than *ABCC6*.[32–36] Finally, it should be noted that the KK/HlJ mice have a number of phenotypic manifestations unrelated to the ectopic mineralization. These include tendency to develop type 2 diabetes, with diabetic nephropathy, as well as interstitial fibrotic heart lesions, corneal degeneration, and fibrous bone lesions.[37–39] (J.P. Sundberg et al, unpublished data). The KK/HlJ mice have also been suggested to develop age-related hearing loss due to homozygosity for mutations in the cadherin 23 gene.[40]

In summary, we have characterized the mineralization aspects of the KK/HlJ mouse strain as a novel model system to study PXE. These mice develop ectopic connective tissue mineralization, similar to that noted in *Abcc6* mutant mice developed by targeted ablation of the corresponding gene. The KK/HlJ mouse strain differs from the *Abcc6*^{tm1JfK} mice in several aspects, including differing degree of mineralization, and a number of associated phenotypes. Note that the genetic alteration in the *Abcc6* gene in KK/HlJ mice is the same as previously noted by Aherrahrou et al[30] in C3H/HeJ mice, yet the phenotypic manifestations are different in several respects. For example, the C3H/HeJ mice do not develop mineralization of the dermal sheath of vibrisse,[41] prominently noted in KK/HlJ mice and also observed in *Abcc6*^{tm1JfK} mice as an early and progressive biomarker of the overall mineralization process.[9] Furthermore, the degree of systemic mineralization is profoundly more severe in KK/HlJ mice than in C3H/HeJ mice (A. Berndt et al, unpublished data), suggesting the influence of modifier genes or epigenetic factors. Thus, it is conceivable that the KK/HlJ mouse will provide novel additional insights into the pathomechanisms of PXE, a currently intractable disease with unknown pathomechanisms that lead to variable phenotypic expression in affected persons.

Acknowledgments

We thank Gerald Harrison for assistance in EDAX and RADAR mapping, Dian Wang for animal care, and Carol Kelly for manuscript preparation.

References

1. Neldner KH, Struk B: Pseudoxanthoma elasticum. Connective Tissue and Its Heritable Disorders: Molecular, Genetic and Medical Aspects. Edited by PM Royce, B Steinmann B. New York, Wiley-Liss, Inc, 2002, pp. 561–583
2. Uitto J, Li Q, Jiang Q: Pseudoxanthoma elasticum: molecular genetics and putative pathomechanisms. J Invest Dermatol 2010, 130:661–670
3. Georgalas I, Papaconstantinou D, Koutsandrea C, Kalantzis G, Karagiannis D, Georgopoulos G, Ladas I: Angioid streaks, clinical course, complications, and current therapeutic management. Ther Clin Risk Manag 2009, 5:81–89
4. Mendelsohn G, Bulkley BH, Hutchins GM: Cardiovascular manifestations of pseudoxanthoma elasticum. Arch Pathol Lab Med 1978, 102:298–302
5. Belinsky MG, Kruh GD: MOAT-E (ARA) is a full-length MRP/cMOAT subfamily transporter expressed in kidney and liver. Br J Cancer 1999, 80:1342–1349
6. Uitto J, Bercovitch L, Terry SF, Terry PF: Pseudoxanthoma elasticum: progress in diagnostics and research towards treatment: summary of the 2010 PXE International Research Meeting. Am J Med Genet 2011, 155A:1517–1526

7. Váradi A, Szabó Z, Pomozi V, de Boussac H, Fülöp K, Arányi T: ABCC6 as a target in pseudoxanthoma elasticum. Curr Drug Targets 2011, 12:671–682
8. Li Q, Jiang Q, Pfendner EG, Váradi A, Uitto J: Pseudoxanthoma elasticum: clinical phenotypes, molecular genetics and putative pathomechanisms. Exp Dermatol 2009, 18:1–11
9. Klement JF, Matsuzaki Y, Jiang Q, Terlizzi J, Choi HY, Fujimoto N, Li K, Pulkkinen L, Birk DE, Sundberg JP, Uitto J: Targeted ablation of the ABCC6 gene results in ectopic mineralization of connective tissues. Mol Cell Biol 2005, 25:8299–8310
10. Gorgels TG, Hu X, Scheffer GL, van der Wal AC, Toonstra J, de Jong PT, van Kuppevelt TH, Levelt CN, de Wolf A, Loves WJ, Scheper RJ, Peek R, Bergen AA: Disruption of Abcc6 in the mouse: novel insight in the pathogenesis of pseudoxanthoma elasticum. Hum Mol Genet 2005, 14:1763–1773
11. Jiang Q, Li Q, Uitto J: Aberrant mineralization of connective tissues in a mouse model of pseudoxanthoma elasticum: systemic and local regulatory factors. J Invest Dermatol 2007, 127:1392–1402
12. Jiang Q, Endo M, Dibra F, Wang K, Uitto J: Pseudoxanthoma elasticum is a metabolic disease. J Invest Dermatol 2009, 129:348–354
13. Jiang Q, Oldenburg R, Otsuru S, Grand-Pierre AE, Horwitz EM, Uitto J: Parabiotic heterogenetic pairing of Abcc6$^{-/-}$/Rag1$^{-/-}$ mice and their wild-type counterparts halts ectopic mineralization in a murine model of pseudoxanthoma elasticum. Am J Pathol 2010, 176:1855–1862
14. LaRusso J, Jiang Q, Li Q, Uitto J: Ectopic mineralization of connective tissue in Abcc6$^{-/-}$ mice: effects of dietary modifications and a phosphate binder - a preliminary study. Exp Dermatol 2008, 17:203–207
15. LaRusso J, Li Q, Jiang Q, Uitto J: Elevated dietary magnesium prevents connective tissue mineralization in a mouse model of pseudoxanthoma elasticum (Abcc6$^{-/-}$). J Invest Dermatol 2009, 129:1388–1394
16. Li Q, LaRusso J, Grand-Pierre AE, Uitto J: Magnesium carbonate-containing phosphate binder prevents connective tissue mineralization in Abcc6$^{-/-}$ mice-potential for treatment of pseudoxanthoma elasticum. Clin Transl Sci 2009, 2:398–404
17. Li Q, Uitto J: The mineralization phenotype in Abcc6$^{-/-}$ mice is affected by Ggcx gene deficiency and genetic background – a model for pseudoxanthoma elasticum. J Mol Med 2010, 88:173–181
18. Sundberg JP, Berndt A, Sundberg BA, Silva KA, Kennedy V, Bronson RT, Yuan R, Paigen B, Harrison DE, Schofield PN: The mouse as a model for understanding chronic diseases of aging: the histopathologic basis of aging in inbred mice. Pathobiol Aging & Age-rel Dis 2011, 1:7179
19. Silva KA, Sundberg JP: Necropsy methods. The Laboratory Mouse. London, Academic Press. 2004
20. Li Q, Jiang Q, LaRusso J, Klement JF, Sartorelli AC, Belinsky MG, Kruh GD, Uitto J: Targeted ablation of Abcc1 or Abcc3 in Abcc6$^{-/-}$ mice does not modify the ectopic mineralization process. Exp Dermatol 2007, 16:853–859
21. Martinez-Hernandez A, Huffer WE: Pseudoxanthoma elasticum: dermal polyanions and the mineralization of elastic fibers. Lab Invest 1974, 31:181–186
22. Kavukcuoglu NB, Li Q, Pleshko N, Uitto J: Connective tissue mineralization in Abcc6$^{-/-}$ mice, a model for pseudoxanthoma elasticum. Matrix Biol 2012, 31:246–252
23. Staats J: Standardized nomenclature for inbred strains of mice: fifth listing. Cancer Res 1972, 32:1609–1646
24. Walker ER, Frederickson RG, Mayes MD: The mineralization of elastic fibers and alterations of extracellular matrix in pseudoxanthoma elasticum. Ultrastructure, immunocytochemistry, and X-ray analysis. Arch Dermatol 1989, 125:70–76
25. Mendell JT, Dietz HC: When the message goes awry: disease-producing mutations that influence mRNA content and performance. Cell 2001, 107:411–414
26. Ivandic BT, Utz HF, Kaczmarek PM, Aherrahrou Z, Axtner SB, Klepsch C, Lusis AJ, Katus HA: New Dysalc loci for myocardial cell necrosis and calcification (dystrophic cardiac calcinosis) in mice. Physiol Genomics 2001, 6:137–144
27. Korff S, Riechert N, Schoensiegel F, Weichenhan D, Autschbach F, Katus HA Ivandic BT: Calcification of myocardial necrosis is common in mice. Virchows Arch 2006, 448:630–638
28. Dellegrottaglie S, Sanz J, Rajagopalan S: Molecular determinants of vascular calcification: a bench to bedside view. Curr Mol Med 2006, 6:515–524
29. Meng H, Vera I, Che N, Wang X, Wang SS, Ingram-Drake L, Schadt EE, Drake TA, Lusis AJ: Identification of Abcc6 as a major causal gene for dystrophic cardiac calcification in mice through integrative genomics. Proc Natl Acad Sci U S A 2007, 104:4530–4535
30. Aherrahrou Z, Doehring LC, Ehlers EM, Liptau H, Depping R, Linsel-Nitschke P, Kaczmarek PM, Erdmann J, Schunkert H: An alternative splice variant in Abcc6, the gene causing dystrophic calcification, leads to protein deficiency in C3H/He mice. J Biol Chem 2008, 283:7608–7615
31. Asano Y, Takashima S, Asakura M, Shintani Y, Liao Y, Minamino T, Asanuma H, Sanada S, Kim J, Ogai A, Fukushima T, Oikawa Y, Okazaki Y, Kaneda Y, Sato M, Miyazaki J, Kitamura S, Tomoike H, Kitakaze M, Hori M: Lamr1 functional retroposon causes right ventricular dysplasia in mice. Nat Genet 2004, 36:123–130
32. Vanakker OM, Martin L, Gheduzzi D, Leroy BP, Loeys BL, Guerci VI, Matthys D, Terry SF, Coucke PJ, Pasquali-Ronchetti I, De Paepe A: Pseudoxanthoma elasticum-like phenotype with cutis laxa and multiple coagulation factor deficiency represents a separate genetic entity. J Invest Dermatol 2007, 127:581–587
33. Li Q, Schurgers LJ, Smith AC, Tsokos M, Uitto J, Cowen EW: Coexistent pseudoxanthoma elasticum and vitamin K-dependent coagulation factor deficiency: compound heterozygosity for mutations in the GGCX gene. Am J Pathol 2009, 174:534–540
34. Li Q, Grange DK, Armstrong NL, Whelan AJ, Hurley MY, Rishavy MA, Hallgren KW, Berkner KL, Schurgers LJ, Jiang Q, Uitto J: Mutations in the GGCX and ABCC6 genes in a family with pseudoxanthoma elasticum-like phenotypes. J Invest Dermatol 2009, 129:553–563
35. Nitschke Y, Baujat G, Botschen U, Wittkampf T, du Moulin M, Stella J, Le Merrer M, Guest G, Lambot K, Tazarourte-Pinturier MF, Chassaing N, Roche O, Feenstra I, Loechner K, Deshpande C, Garber SJ, Chikarmane R, Steinmann B, Shahinyan T, Martorell L, Davies J, Smith WE, Kahler SG, McCulloch M, Wraige E, Loidi L, Höhne W, Martin L, Hadj-Rabia S, Terkeltaub R, Rutsch F: Generalized arterial calcification of infancy and pseudoxanthoma elasticum can be caused by mutations in either ENPP1 or ABCC6. Am J Hum Genet 2012, 90:25–39
36. Li Q, Schumacher W, Siegel D, Jablonski D, Uitto J: Cutaneous features of pseudoxanthoma elasticum in a patient with generalized arterial calcification of infancy due to homozygous missense mutation in the ENPP1 gene. Br J Dermatol 2012, 166:1107–1111
37. Ikeda H: KK mouse. Diabetes Res Clin Pract 1994, 24(Suppl): S313–S316
38. Shimada T: Correlation between metabolic and histopathological changes in the myocardium of the KK mouse. Effect of diltiazem on the diabetic heart. Jpn Heart J 1993, 34:617–-626
39. Lu G, Uga S, Miyata M, Ishikawa S: Histopathological study of congenitally diabetic yellow KK mouse lens. Jpn J Ophthalmol 1993, 37:369–378
40. Zheng QY, Johnson KR, Erway LC: Assessment of hearing in 80 inbred strains of mice by ABR threshold analyses. Hear Res 1999, 130:94–107
41. Le Corre Y, Le Saux O, Froeliger F, Libouban H, Kauffenstein G, Willoteaux S, Leftheriotis G, Martin L: Quantification of the calcification phenotype of Abcc6$^{-/-}$ deficient mice with microcomputed tomography. Am J Pathol 2012, 180:2208–2213